Multiple white matter lesions combined with subcortical microbleeds in patients with intravascular large B-cell lymphoma

Han Xu[1]^, Jia-Cun Li[1]^, Liang-Jie Lin[2]^, Xiao-Hui Liu[3]^, Tao Gu[4]^, Xiao-Ming Zhang[5], Xi-Ming Wang[1]^, Tao Gong[1#]^, Jian-Jun Xiu[1#]^

[1]Department of Radiology, Shandong Provincial Hospital Affiliated to Shandong First Medical University, Jinan, China; [2]Philips Healthcare, Beijing, China; [3]Department of Neurology, Shandong Provincial Hospital Affiliated to Shandong First Medical University, Jinan, China; [4]Department of Radiology, Beijing Hospital, National Center of Gerontology, Institute of Geriatric Medicine, Chinese Academy of Medical Sciences, Beijing, China; [5]Department of Radiology, Qilu Hospital, Cheeloo College of Medicine, Shandong University, Jinan, China

[#]These authors contributed equally to this work.

Correspondence to: Jian-Jun Xiu, MD, PhD. Department of Radiology, Shandong Provincial Hospital Affiliated to Shandong First Medical University, 324 Jingwu Weiqi Road, Huaiyin District, Jinan 250021, China. Email: 15168889129@163.com; Tao Gong, MD, PhD. Department of Radiology, Shandong Provincial Hospital Affiliated to Shandong First Medical University, 324 Jingwu Weiqi Road, Huaiyin District, Jinan 250021, China. Email: haitao880801@126.com.

Introduction

Intravascular large B-cell lymphoma (IVLBCL) is a rare subtype of non-Hodgkin's lymphoma, which was updated and revised in the World Health Organization (WHO) classification of lymphatic neoplasms in 2017 and classified as an independent subtype of extranodal diffuse large B-cell lymphoma (1-4). The main pathological features of IVLBCL are proliferation of lymphoma cells in the lumen of capillaries, small- and medium-sized vessels, leading to occlusions and subsequent changes. Most cases of IVLBCL are not diagnosed until postmortem because of variable clinical presentation and non-specific laboratory findings (5-7).

Signs and symptoms of IVLBCL are attributed to vascular occlusion. According to some case series reports, 80% of patients have central nervous system (CNS) involvement, but it is rarely limited to this system, and usually does not involve lymph nodes or peripheral blood (2). More than half

of patients with IVLBCL develop cerebrovascular events, cognitive impairment, spatial disorientation, transient ischemic attacks, and seizures (8,9). Neuroimaging findings vary widely in patients with IVLBCL, ranging from normal findings to hyperintense lesions in the pons on T2-weighted imaging (T2WI), meningeal thickening and abnormal enhancement, infarct-like lesions, and non-specific white matter lesions (6,9,10).

Because of the wide variation in clinical presentation and non-specific brain magnetic resonance imaging (MRI) findings, accurate diagnosis and early treatment of IVLBCL remain difficult (5,11). In this study, the clinical data and imaging characteristics of 4 IVLBCL patients were summarized and analyzed to further improve radiologists and clinicians' understanding of the disease.

Case presentations

All procedures performed in this study were in accordance

^ ORCID: Han Xu, 0000-0003-0687-0771; Jia-Cun Li, 0000-0002-2961-1951; Liang-Jie Lin, 0000-0002-3174-3136; Xiao-Hui Liu, 0000-0002-4901-1881; Tao Gu, 0000-0002-3110-2152; Xi-Ming Wang, 0000-0002-1213-1003; Tao Gong, 0000-0001-9689-0420; Jian-Jun Xiu, 0000-0003-4256-9935.

8808

Xu et al. Unusual MRI pattern in intravascular large B-cell lymphoma

Table 1 Laboratory examination-related indicators of four patients

Laboratory findings	Case 1	Case 2	Case 3	Case 4
Hb (g/L) (130–175)	127↓	267↑	–	185.0↑
RBC (10^{12}/L) (4.3–5.8)	4.09↓	5.01	–	7.36↑
PLT (10^9/L) (125–350)	164	267	–	149
WBC (10^9/L) (3.5–9.5)	4.09	6.19	–	5.96
ESR (mm/h) (0–20)	7	27↑	–	23↑
LDH (U/L) (120–250)	359.70↑	597.50↑	–	641↑
CRP (mg/L) (0–10)	13.11↑	4.21	–	–
ALT (U/L) (9–50)	28	44	–	12
AST (U/L) (15–40)	18	37	–	32
BMG (mg/L) (1.0–3.0)	2.51	1.70	–	–
D-dimer (mg/L) (<0.5)	0.10	0.50↑	–	0.55↑
CSF-Pro (g/L) (0.15–0.45)	2.36↑	1.33↑	1.01↑	0.55↑

Hb, hemoglobin; RBC, red blood cell; PLT, platelet; WBC, white blood cell; ESR, erythrocyte sedimentation rate; LDH, lactate dehydrogenase; CRP, C-reactive protein; ALT, alanine aminotransferase; AST, aspartate aminotransferase; BMG, beta-2 microglobulin; D-dimer, D2 polymers; CSF-Pro, cerebrospinal fluid protein. "↑" means above the normal range, and "↓" means below the normal range.

with the ethical standards of the institutional and/or national research committee(s) and with the Helsinki Declaration (as revised in 2013). Written informed consent was provided by the 4 patients for publication of the case reports and accompanying images. A copy of the written consent is available for review by the editorial office of this journal.
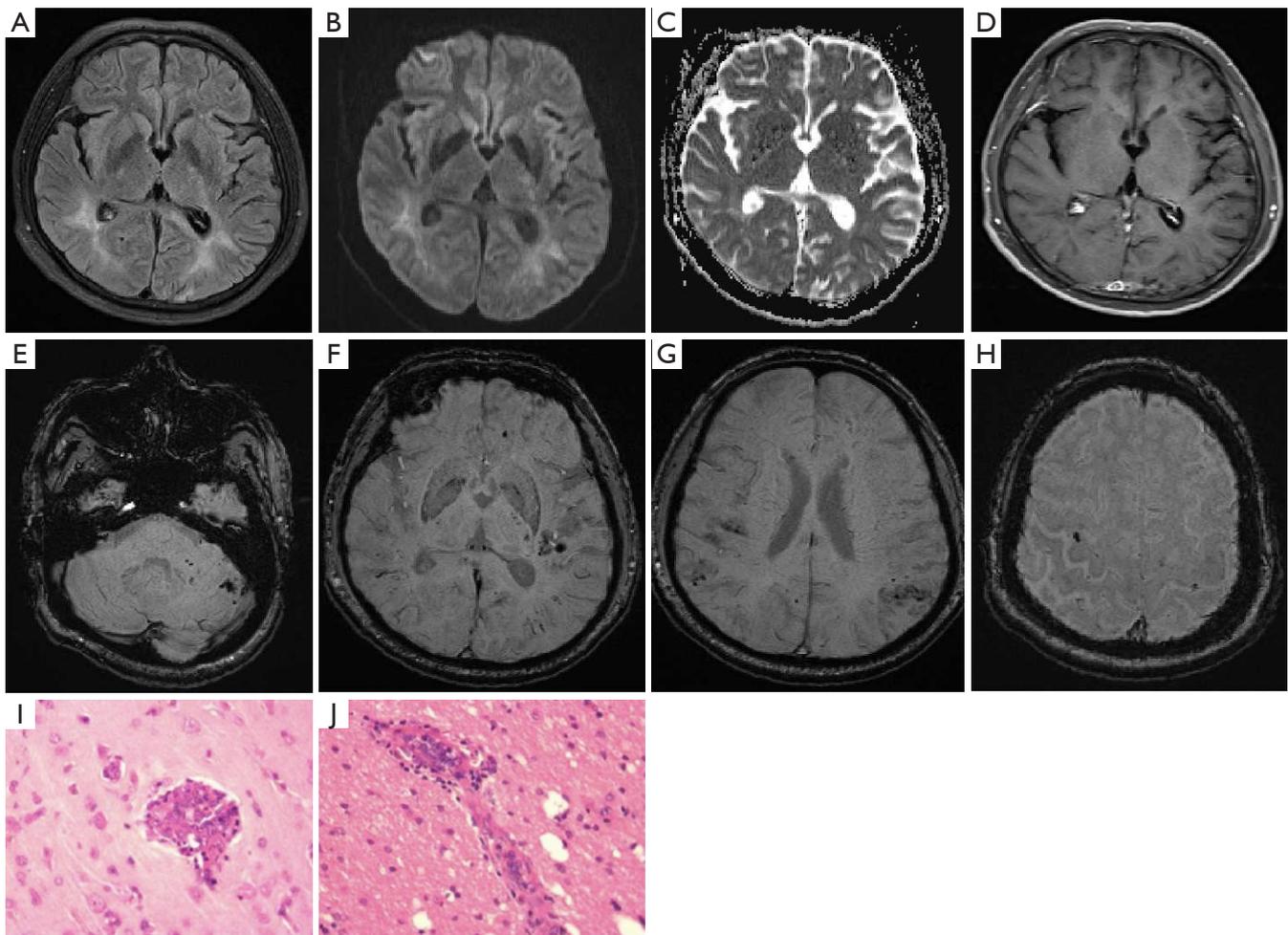
Case 1

A 56-year-old male with a lengthy medical history of recurrent episodes of lower limb weakness and back pain following a fall on the stairs 16 months prior, as well as a history of stroke for 8 months, initially presented to our department with a sudden onset of coma, accompanied by seizures. The patient's memory had deteriorated significantly since the onset of the disease. There was no lymphadenopathy, hepatosplenomegaly, or rash on examination. Also, no fever, nausea, or vomiting was observed during the treatment.

Blood routine examination (BRE) showed a mild decrease in red blood cell count and hemoglobin count, without leukocytosis or thrombocytopenia and erythrocyte sedimentation (ESR) rate was normal. Lactate dehydrogenase (LDH) and C-reactive protein (CRP) were elevated to

359.70 U/L and 13.11 mg/L, respectively, whereas alanine aminotransferase (ALT), aspartate aminotransferase (AST), and beta-2 microglobulin (BMG) were within normal limits. The D-dimer was normal and cerebrospinal fluid (CSF) analysis revealed an elevated protein level (*Table 1*).

Cranial MRI showed abnormal signals in the bilateral brain parenchyma, involving supratentorial and infratentorial areas, including the periventricular white matter, frontal lobe, parietal lobe, splenium of corpus callosum, basal ganglia, left cerebellum, and left cerebral peduncle. MRI showed diffuse hypointensity on T1-weighted imaging (T1WI), hyperintensity on T2-weighted imaging (T2WI) and T2-fluid attenuated inversion-recovery (T2-FLAIR) imaging (*Figure 1A*). On diffusion-weighted imaging (DWI, b value =1,000 s/mm^2), these lesions were partially hyperintense, but the corresponding apparent diffusion coefficient (ADC) signal was not reduced (*Figure 1B,1C*). Contrast enhancement scanning with diethylenetriamine penta-acetic acid (Gd-DTPA) revealed no significant abnormal enhancement (*Figure 1D*). Susceptibility-weighted imaging (SWI) showed multiple punctate to small clusters of microbleeds in the subcortical areas of the bilateral cerebral hemispheres, cerebellum, basal ganglia, and thalamus (*Figure 1E-1H*). The patient's physical examination revealed cognitive decompensation,

Figure 1 A 56-year-old male's images (case 1). (A) Hyperintense lesions in the periventricular white matter on T2-FLAIR. (B,C) DWI (b value =1,000 s/mm^2) showed multiple high-intensity in the periventricular white matter, and the corresponding ADC was not reduced. (D) T1 enhancement scan has no abnormal enhancement in brain parenchyma. (E-H) SWI showed patchy of hypointensity in the subcortical areas. (I,J) Pathologic specimen showed perivascular lymphocytic infiltration, and small vessels filled with uniformly bulky lymphocytes (hematoxylin-eosin, ×400). T2-FLAIR, T2 fluid-attenuated inversion recovery; DWI, diffusion-weighted imaging; ADC, apparent diffusion coefficient; SWI, susceptibility-weighted imaging.

and the localization diagnosis was limbic system, cortical, or diffuse white matter lesions. MRI revealed multiple abnormal signals in the brain's subcortex, more than ever before, and inflammatory demyelinating lesions were suspected. The patient received aspirin and clopidogrel therapy for anti-platelet aggregation, along with a statin, which were aimed at improving brain microcirculation. Furthermore, symptomatic treatments, including nutritional support and interventions targeting cognitive impairment, were administered. The patient's condition worsened during

treatment and a brain biopsy was performed.

This patient's brain biopsy revealed perivascular lymphocytic infiltration, myelin degradation, small vessel hyperplasia, and glial cell hyperplasia. The small vessels were filled with consistently larger lymphocytes (*Figure 1I,1J*). Tumor cells were positive for commonly used B-cell markers (CD20, CD79α, and PAX-5), and other B-cell markers (MUM1, Bcl-2, and Bcl-6), and negative for T-cell markers (CD3 and CD7) by immunohistochemical staining, consistent with a diagnosis of IVLBCL. The Ki-67

8810

Xu et al. Unusual MRI pattern in intravascular large B-cell lymphoma

labeling was approximately 80%.

Case 2

A 60-year-old man was referred to Shandong Provincial Hospital with a history of gait instability, recurrent dizziness, generalized weakness, and numbness of the limbs, accompanied by nausea and vomiting for 2 weeks. The patient had poor mental health, hallucinations, and weight loss since the condition first manifested. The weight loss was significant, at 7–8 kg over 2 weeks. He also had a history of hypertension and diabetes mellitus.

Laboratory workup revealed an elevated LDH level, whereas CRP, ALT, AST, and BMG were within normal limits. CSF analysis revealed an elevated protein level. BRE was normal and ESR was elevated to 27 mm/h (*Table 1*).

Brain MRI showed multiple hypointense lesions on T1WI, and hyperintense lesions on T2WI and T2-FLAIR in the bilateral frontal lobe, parietal lobe, occipital lobe, left temporal lobe, splenium of corpus callosum, and bilateral cerebellar hemispheres (*Figure 2A*). These lesions showed hyperintensity on DWI and reduced signal intensity on the corresponding ADC (*Figure 2B*,*2C*), whereas T2WI and T2-FLAIR showed a more extensive and heterogeneous lesion than on DWI (*Figure 2D-2F*). Patchy abnormal enhancement was seen locally in the right frontal lobe, as well as thickening and linear enhancement of the right meningeal and subcortical gyrus-like enhancement (*Figure 2G-2I*). This patient's condition has been recurrent, and the presence of multiple abnormal MRI signals suggests a potential occurrence of acute-subacute infarction. The patient received a combination of aspirin and clopidogrel as dual anti-treatment, along with a statin, antihypertensive medication, hypoglycemic agents, treatments to improve cerebral circulation, as well as nutritional and psychiatric symptomatic treatment for 2 months. Later, during the follow-up, there was an occurrence of memory loss and worsening of the patient's condition. Consequently, a brain tissue biopsy was performed.

Pathologic specimen showed perivascular lymphocytic and invasion of brain tissue, and small vessels filled with uniformly bulky lymphocytes (*Figure 2J*,*2K*).

Case 3

A 67-year-old man presented with a history of dizziness, weakness of both lower extremities, with gait instability for 6 months. Subsequent head MRI revealed multiple subacute cerebral infarctions. A computed tomography (CT) angiography of the head and neck showed severe stenosis of the internal carotid artery. The patient underwent angioplasty and stent placement. Although symptoms of dizziness and bilateral lower limb weakness persisted, there was some improvement compared to the initial onset. However, the patient was admitted 2 months ago due to worsening symptoms.

Laboratory tests suggested an elevated CSF protein concentration of 1.01 g/L (*Table 1*).

Multiple hypointense lesions on T1WI, hyperintense lesions on T2WI, and T2-FLAIR in the bilateral frontal lobe, parietal lobe, occipital lobe, temporal lobe, corpus callosum, periventricular white matter, and left basal ganglia were found on brain MRI (*Figure 3A*,*3B*). DWI and ADC maps show partial diffusion restriction in these lesions (*Figure 3C*,*3D*). In brain parenchyma, there was patchy abnormal enhancement (*Figure 3E*). SWI showed numerous punctate to small clusters of microbleeds in the subcortical areas of the bilateral cerebral hemispheres (*Figure 3F-3H*). After stenting, the patient developed lower limb weakness and aggravated dizziness symptoms. The intravenous infusion of high doses of methylprednisolone led to a reduction in brain lesions within a short time. Aspirin and clopidogrel were continued, as were lipid-lowering and circulatory drugs, but the symptoms did not improve. The symptoms were still present during regular follow-up after the brain biopsy.

Brain tissue biopsy suggested that few large cell infiltrates in local small vessels were seen (*Figure 3I*). These cells were stained strongly with CD20 (*Figure 3J*) and were negative for CD3, with strong diffuse nuclear staining with Bcl-2, focally positive MUM1 staining, and negative for CD10 and Bcl-6 staining.

Case 4

A 31-year-old woman presented to Shandong Provincial Hospital with a 3-month long headache and 2 days of impaired consciousness due to episodic limb twitching. The patient's headache began to worsen 1 month prior to admission, with blurred vision and unresponsiveness.

BRE demonstrated an increase in the number of red blood cell counts and hemoglobin counts, and the D-dimer was increased to 0.55 mg/L. CSF analysis showed an increase in CSF protein to 0.55 g/L. External hospital examination indicated LDH was elevated to 641 U/L (*Table 1*).
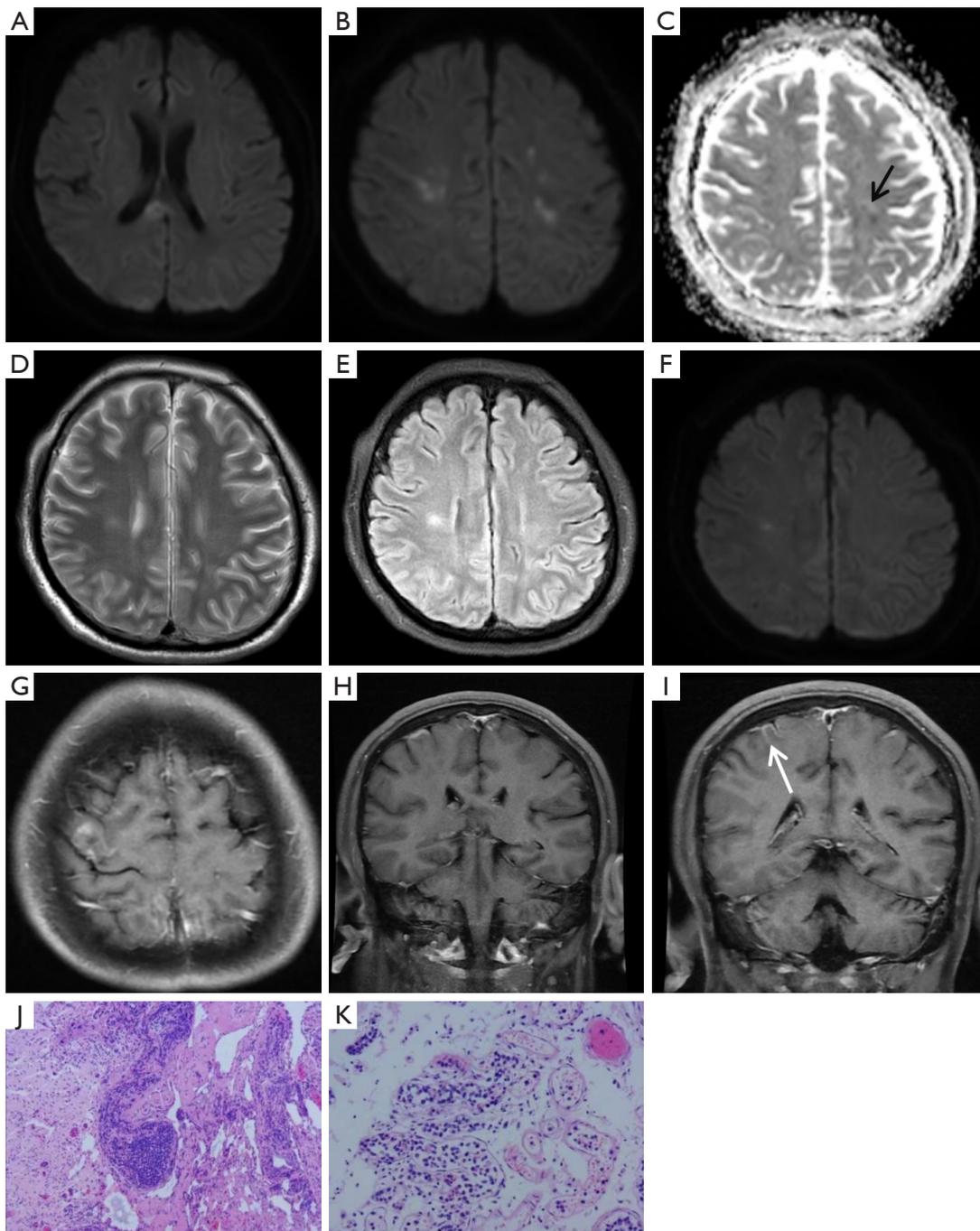
Figure 2 Images of a 60-year-old male (case 2). (A,B) DWI (b value =1,000 s/mm^2) showed multiple patches of hyperintensity in corpus callosum and bilateral cerebral hemispheres. (C) The corresponding ADC map showed that some of these lesions were high-intensity, and some were low-intensity (black arrow). (D,E) T2WI and T2-FLAIR showed focal hyperintensity in the right radial crown area. (F) The lesion of radial crown area appeared to be larger on T2WI than on DWI. (G) In image, gadolinium-enhanced T1-weighted imaging revealed abnormal enhancement in the right frontal lobe. (H) Image illustrated thickening and linear enhancement of the right meninges. (I) Subcortical gyrus-like enhancement. (J,K) Pathologic specimen showed perivascular lymphocytic and invasion of brain tissue, and small vessels filled with uniformly bulky lymphocytes (hematoxylin-eosin, ×400). DWI, diffusion-weighted imaging; ADC, apparent diffusion coefficient; T2WI, T2-weighted imaging; T2-FLAIR, T2 fluid-attenuated inversion recovery; T1WI, T1-weighted imaging.
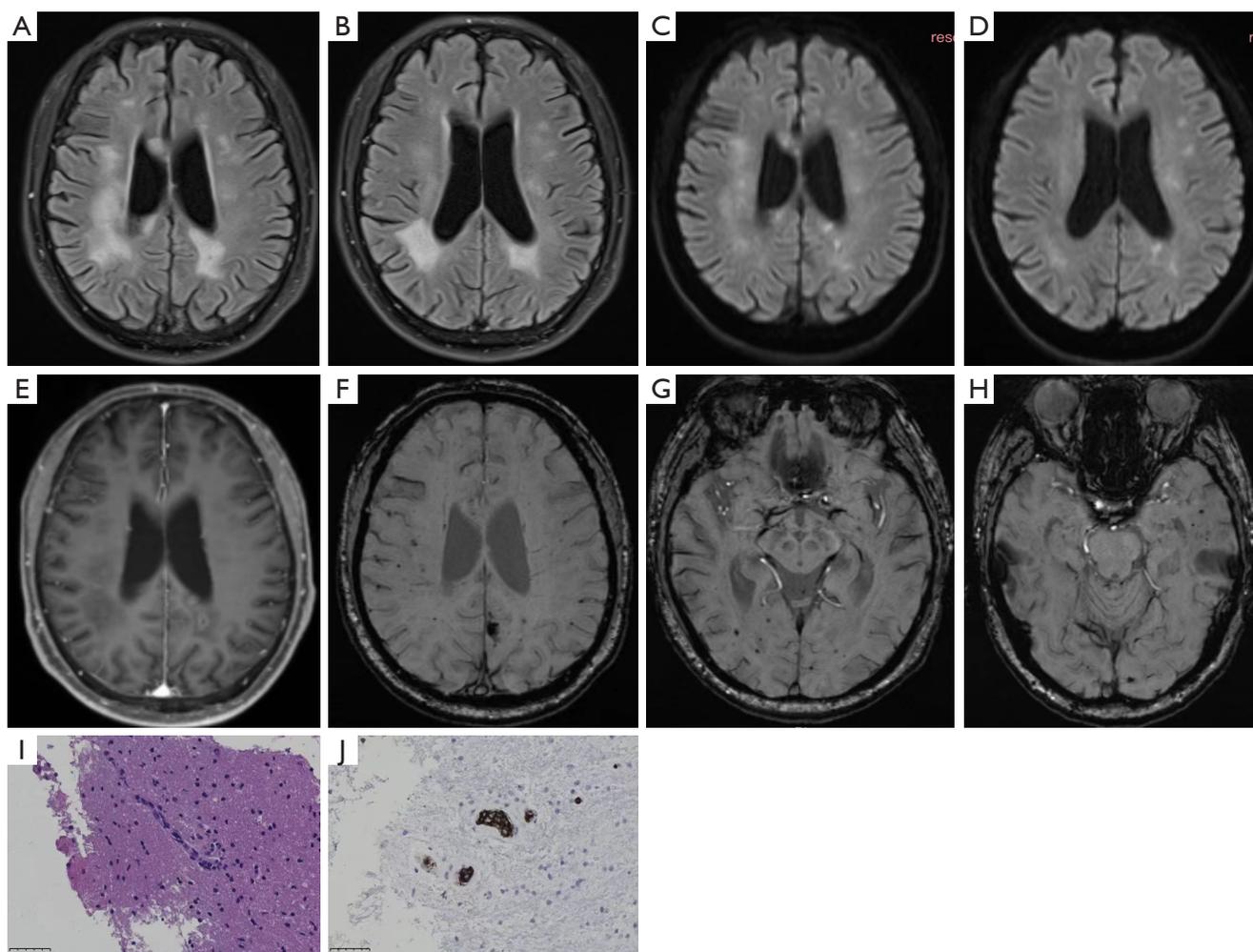
Figure 3 Images of a 67-year-old male (case 3). (A,B) T2-FLAIR showed multiple patches of hyperintensity lesions in corpus callosum and bilateral cerebral hemispheres. (C,D) The corresponding DWI (b value =1,000 s/mm^2) showed that some of these lesions were high-intensity. (E) Gadolinium-enhanced T1WI showed abnormal enhancement of periventricular white matter. (F-H) SWI showed numerous punctate to small clusters of microbleeds in the subcortical areas of the bilateral cerebral hemispheres. (I) Optical microscopy findings showed tumor cells were restricted to intravascular spaces (hematoxylin-eosin, ×200). (J) Optical microscopy findings showed membrane of tumor cells were positive for CD20 (×200). T2-FLAIR, T2 fluid-attenuated inversion recovery; DWI, diffusion-weighted imaging; T1WI, T1-weighted imaging; SWI, susceptibility-weighted imaging.

The MRI revealed a large area of hyperintensity on T1WI with a corresponding hypointensity on T2WI, surrounded by patchy edema in the bilateral cerebral hemispheres and right cerebellar hemisphere (*Figure 4A-4C*). There were some lesions that did not show hyperintensity on DWI (*Figure 4D,4E*). SWI demonstrated numerous microbleeds and superficial siderosis in the cortical and subcortical white matter of the bilateral cerebral hemispheres (*Figure 4F,4G*). Following a contrast enhancement scan with Gd-DTPA, the brain parenchyma showed diffuse abnormal enhancement

(*Figure 4H*). Cyclophosphamide was administered through intravenous infusion, along with methylprednisolone therapy. Subsequently, the treatment was transitioned to oral administration of prednisolone. Hormone therapy yielded in partial alleviation of symptoms; however, symptoms experienced a resurgence upon cessation of hormone treatment. Cerebral bleeding and lung infection happened following the brain biopsy, and the patient's condition quickly deteriorated. She was sent back to the neighborhood hospital for treatment after the operation,
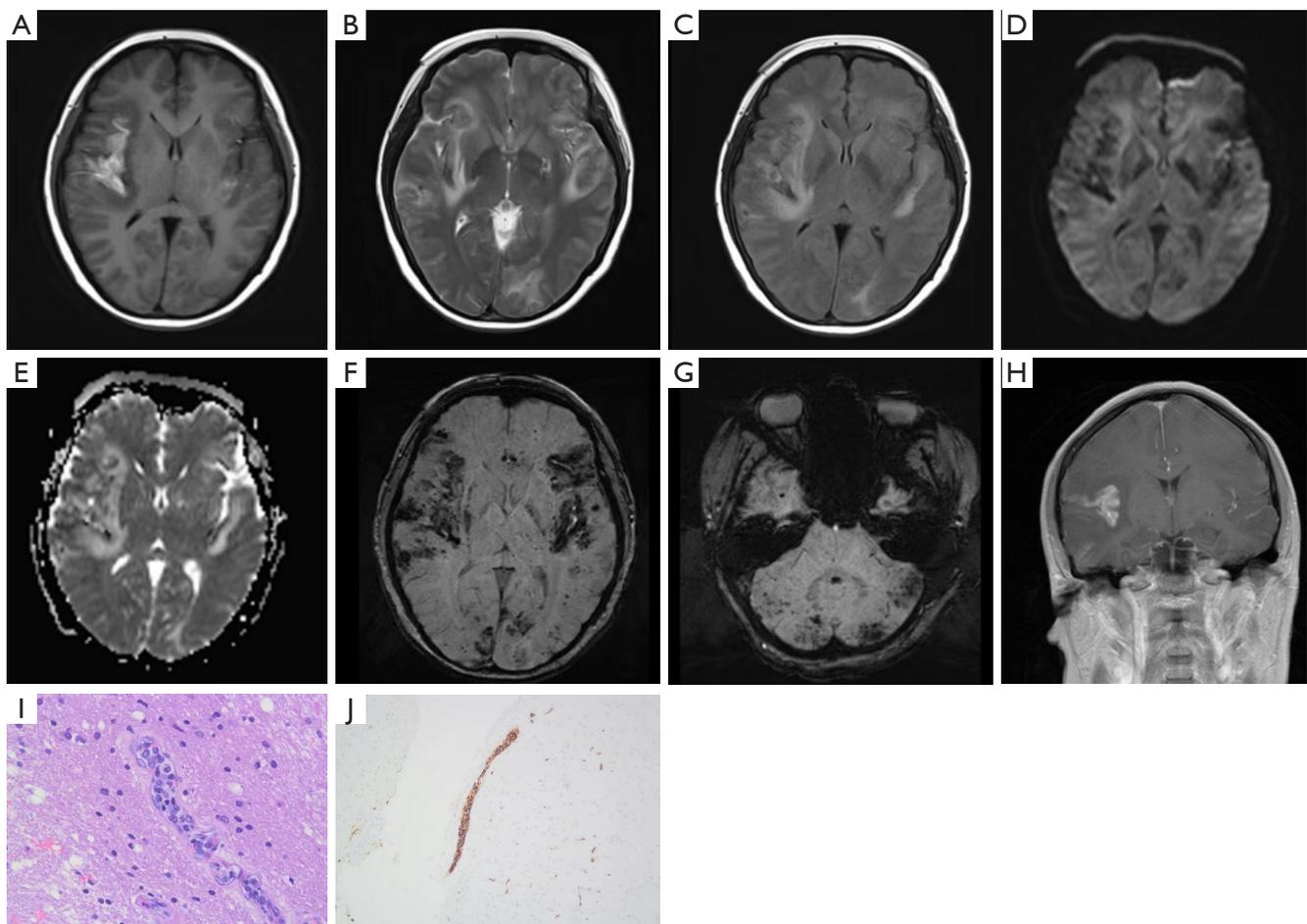
Figure 4 Images of a 31-year-old female (case 4). (A-C) Corresponding to T1WI (A), T2WI and T2-FLAIR, respectively, showing diffuse patchy hyperintensity and hypointensity in the cerebral hemispheres bilaterally with edema of the surrounding brain tissue. (D,E) No significant diffusion restriction seen on DWI (b value =1,000 s/mm^2) and ADC. (F,G) Multiple low-intensity in the bilateral cerebral and cerebellum can be seen on SWI. (H) Gadolinium-enhanced T1WI showed an enhanced lesion. (I) Pathologic specimen showed that there was exudation and edema around the small vessels, and a large number of heterogeneous lymphocyte aggregates were seen in the lumen of the small vessels (hematoxylin-eosin, ×400). (J) Immunohistochemical staining showed: tumor cells CD79α(+) (×200). T1WI, T1-weighted imaging; T2WI, T2-weighted imaging; T2-FLAIR, T2 fluid-attenuated inversion recovery; DWI, diffusion-weighted imaging; ADC, apparent diffusion coefficient; SWI, susceptibility-weighted imaging.

where she later passed away. The illness lasted for longer than 5 months in total.

The brain biopsy's histology revealed capillary hyperplasia in the white matter, as well as hemorrhage, exudation, and edema around small vessels. Atypical lymphoid cell proliferation was observed in the lumen of small vessels in the brain and meningeal surface (*Figure 4I*), with positive immunoreactivity for CD79α (*Figure 4J*) and CD20 in the small capillaries, leading to the diagnosis of intravascular large B-cell lymphoma. There was no immunoreactivity for CD2, CD3, CD8, CD10, or CD30. The Ki-67 stain showed a proliferative index of approximately 70%.

Discussion

IVLBCL is a rare systemic lymphoproliferative disorder characterized by selective infiltration of lymphoid cells in blood vessels. It exhibits striking angiotropic growth, which results in a variety of clinical presentations and extremely heterogeneous MRI findings depending on the

location of the vascular occlusions (12-14). We found that the white matter lesions caused by tumor cell intravascular infiltration primarily affect small vessels rather than the cerebrovascular distribution of classic gray-white matter infarctions. Furthermore, the SWI frequently showed multiple subcortical microbleeds along the small vessels.

The most common MRI findings are hyperintensity lesions on T2WI and T2-FLAIR with bilateral white matter involvement, and some of them may show diffusion restriction on DWI and ADC maps, which is consistent with the results of previous studies (5,8,10). The brain MRI findings of IVLBCL were classified into the following patterns: hyperintense lesions in the pons on T2WI, meningeal thickening or abnormal enhancement, infarct-like lesions, and non-specific white matter lesions (7,11,12). The most common of these abnormal findings was an infarct-like lesion (14). Unlike common cerebral infarcts (atherosclerosis, cardiogenic embolism, etc.), the infarct-like lesions seen in this group of cases were mostly located in bilateral cerebral white matter, symmetrically distributed, and not in accordance with typical infarcts in the vascular distribution area. Although the patients with cerebral infarcts typically exhibit restricted diffusion with low signal intensity on ADC images; the presented cases in this group demonstrated hyperintense lesions on DWI, with only mild corresponding ADC signal reduction, generally equivalent to or higher than the signal intensity. The cerebrovascular distribution of these white matter lesions differs from that of common cerebral infarct-like lesions. This may be related to the existence of tumor cells in small vessels without widespread in the peripheral blood. The pathophysiological mechanisms underlying the characteristic pattern of selective lymphoma cell growth in the vascular lumen are unknown, but a possible explanation is a disruption in intercellular adhesion molecules, which keeps lymphocytes fixed in the initial position rather than spreading widely with the peripheral blood circulation (15,16). There were 3 cases of the T2WI high-intensity lesions exhibiting punctate or patchy enhancement within the lesions, which suggested that the tumor cells had penetrated the extravascular brain parenchyma, which is uncommon in typical cerebral infarction; multiple focal white matter abnormal signals are visible on MRI, which differs from the classical gray-white matter distribution. It has also been explained in the literature that microdefects in the parenchyma or sluggish flow in the lumen of capillaries, small veins, and arteries may be responsible for their bias towards involvement of the periventricular white matter, which is not attributed to any

vascular territory (6). The MRI appearance of intravascular lymphomatosis may also manifest as meningeal thickening and abnormal parenchymal enhancement which is likely due to lymphoma cell extravascular invasion (10). In conclusion, the selective infiltration of lymphoma cells within the vasculature, as well as varying degrees of cellular infiltration, resulted in different imaging patterns in IVLBCL patients.

Most importantly, in our cases, multiple microhemorrhages with subcortical distribution along small vessels were found in all 3 patients who underwent SWI sequences. One of them had a large patchy hyperintensity on T1WI with a large edema signal in the surrounding brain tissue, indicating subacute early hemorrhage. On SWI, the other patients had scattered hypointensity, indicating a chronic phase of hemorrhage. In contrast, microhemorrhages in hypertensive patients primarily distribute in the basal ganglia, brainstem, and thalamus. On the other hand, microhemorrhages in amyloid cerebrovascular disease are commonly found in the cerebral cortex and subcortical regions, particularly in the occipital, temporal, and parietal lobes. They are less frequently observed in the brainstem and cerebellum. When considering the possibility of IVLBCL, it is important to note the presence of multiple white matter lesions involving small blood vessels in the brain. These lesions are often accompanied by multiple subcortical microhemorrhages along small blood vessels.

Previous cases have described multiple microhemorrhagic lesions and large bleeding accompanied by symptoms of neural detachment (9,17,18). The mechanism of hemorrhage in IVLBCL is still unknown. We speculated that the hemorrhage may be caused by chronic degenerative or inflammatory changes and fibrin necrosis in the vessel wall resulting from the direct interaction of atypical lymphocytes with cerebrovascular endothelial cells (9,17,19), and that this injury to the vessel wall can lead to dilatation of the vessel, microaneurysm formation, and finally hemorrhage. Also, luminal narrowing and occlusion can occur if lymphoma cells infiltrate the vessel wall. Blood stasis and venous infarction occur in capillaries and small veins, which may lead to hemorrhagic lesions (20) and progressive edema or venous infarction in the surrounding tissues.

This study has several limitations, with its small sample size being the greatest deficiency due to the rarity of this disease. Although the brain MRI presentation was diverse, all reflected a growth pattern of selective intravascular infiltration of lymphoma cells. Only 3 cases were examined with SWI, but all showed distribution along the subcortical vessels. Due to the relatively poor clinical prognosis of

IVLBCL, there was also no follow-up MRI examination in our cohort. In conclusion, the vascular distribution of white matter lesions in IVLBCL differs from that of classic gray-white matter infarctions, and multiple subcortical microbleeds along small vessels should be considered as a possibility of IVLBCL. It is critical to recognize that these MRI patterns may indicate selective and varying degrees of vascular invasion by tumor cells, and that timely recognition of these imaging patterns may lead to an early diagnosis of IVLBCL with a better prognosis.

Footnote

Conflicts of Interest: All authors have completed the ICMJE uniform disclosure form (available at https://qims.amegroups.com/article/view/10.21037/qims-23-528/coif). LJL is an employee of Philips Healthcare. The other authors have no conflicts of interest to declare.

Ethical Statement: The authors are accountable for all aspects of the work in ensuring that questions related to the accuracy or integrity of any part of the work are appropriately investigated and resolved. All procedures performed in this study were in accordance with the ethical standards of the institutional and/or national research committee(s) and with the Helsinki Declaration (as revised in 2013). Written informed consent was provided by the 4 patients for publication of the case reports and accompanying images. A copy of the written consent is available for review by the editorial office of this journal.

Open Access Statement: This is an Open Access article distributed in accordance with the Creative Commons Attribution-NonCommercial-NoDerivs 4.0 International License (CC BY-NC-ND 4.0), which permits the non-commercial replication and distribution of the article with the strict proviso that no changes or edits are made and the original work is properly cited (including links to both the formal publication through the relevant DOI and the license). See: https://creativecommons.org/licenses/by-nc-nd/4.0/.

References

1. Barker JL, Swarup O, Puliyayil A. Intravascular large B-cell lymphoma: representative cases and approach to diagnosis. BMJ Case Rep 2021;14:e244069.
2. Grimm KE, O'Malley DP. Aggressive B cell lymphomas in the 2017 revised WHO classification of tumors of hematopoietic and lymphoid tissues. Ann Diagn Pathol 2019;38:6-10.
3. Kaito S, Muto H, Miyawaki S, et al. Timely Diagnosis and Successful Treatment of Intravascular Large B-Cell Lymphoma in an Elderly Patient with Poor Performance Status. Am J Case Rep 2019;20:780-4.
4. Ponzoni M, Campo E, Nakamura S. Intravascular large B-cell lymphoma: a chameleon with multiple faces and many masks. Blood 2018;132:1561-7.
5. Abe Y, Narita K, Kobayashi H, et al. Clinical value of abnormal findings on brain magnetic resonance imaging in patients with intravascular large B-cell lymphoma. Ann Hematol 2018;97:2345-52.
6. Liew CL, Shyu WC, Tsao WL, et al. Intravascular lymphomatosis mimicks a cerebral demyelinating disorder. Acta Neurol Taiwan 2006;15:264-8.
7. Orwat DE, Batalis NI. Intravascular large B-cell lymphoma. Arch Pathol Lab Med 2012;136:333-8.
8. Matsue K, Abe Y, Narita K, et al. Diagnosis of intravascular large B cell lymphoma: novel insights into clinicopathological features from 42 patients at a single institution over 20 years. Br J Haematol 2019;187:328-36.
9. Passarin MG, Wen PY, Vattemi E, et al. Intravascular lymphomatosis and intracerebral haemorrhage. Neurol Sci 2010;31:793-7.
10. Yamamoto A, Kikuchi Y, Homma K, et al. Characteristics of intravascular large B-cell lymphoma on cerebral MR imaging. AJNR Am J Neuroradiol 2012;33:292-6.
11. Yoon SE, Kim WS, Kim SJ. Asian variant of intravascular large B-cell lymphoma: a comparison of clinical features based on involvement of the central nervous system. Korean J Intern Med 2020;35:946-56.
12. Williams RL, Meltzer CC, Smirniotopoulos JG, et al. Cerebral MR imaging in intravascular lymphomatosis. AJNR Am J Neuroradiol 1998;19:427-31.
13. Glass J, Hochberg FH, Miller DC. Intravascular lymphomatosis. A systemic disease with neurologic manifestations. Cancer 1993;71:3156-64.
14. Richie MB, Guterman EL, Shah MP, et al. Susceptibility-Weighted Imaging of Intravascular Lymphoma of the Central Nervous System. JAMA Neurol 2022;79:86-7.

15. Haninger DM, Davis TA, Parker JR, et al. Intravascular large B-cell lymphoma presenting as acute hemorrhagic cerebral infarct with delirium. Ann Clin Lab Sci 2013;43:305-10.

16. Ponzoni M, Arrigoni G, Gould VE, et al. Lack of CD 29 (beta1 integrin) and CD 54 (ICAM-1) adhesion molecules in intravascular lymphomatosis. Hum Pathol 2000;31:220-6.

17. Leclercq L, Mechtouff L, Hermier M, et al. Intravascular large B-cell lymphoma mimicking cerebral amyloid angiopathy-related inflammation. Rev Neurol (Paris) 2018;174:265-6.

18. Kimura M, Fujiwara S, Tanaka A, et al. Multiple Cerebral Hemorrhages With Microbleeds in Intravascular Large B-Cell Lymphoma. J Stroke Cerebrovasc Dis 2020;29:104798.

19. Uzuka T, Higuchi F, Matsuda H, et al. Intravascular Lymphoma with an Acute Course of Cerebellar Hemorrhage: A Case Report. Neurol Med Chir (Tokyo) 2018;58:96-100.

20. Yaura K, Watanabe G, Nakamura T, Tsukita K, Suzuki H, Suzuki Y. Intravascular large B-cell lymphoma with multiple intracranial hemorrhages diagnosed by brain biopsy. Rinsho Shinkeigaku 2020;60:206-12.